Chemie der Erde 77 (2017) 625–631

Contents lists available at ScienceDirect

Chemie der Erde

journal homepage: www.elsevier.de/chemer

Trace elements indicating humid climatic events in the Ordovician–early Silurian

Enli Kiipli, Tarmo Kiipli*, Toivo Kallaste, Siim Pajusaar

Department of Geology at Tallinn University of Technology, Ehitajate tee 5, 19086 Tallinn, Estonia

ARTICLE INFO

Article history:
Received 27 January 2017
Received in revised form 23 May 2017
Accepted 29 May 2017
Editorial handling - Carita Augustsson

Keywords:
Ordovician
Silurian
Palaeoclimate
Baltica
Clay
Rb
Zr
Nb
Ti

ABSTRACT

The chemical composition of the clay fraction separated from the carbonate rock of the north-eastern Baltoscandian Basin was analysed and interpreted. Increased contents of Rb, Zr, Nb, Ti and their Al_2O_3-normalised ratios were detected at several stratigraphical levels in the geological sections of the Middle Ordovician–Upper Llandovery. In the weathering areas, Rb, Zr, Nb, Ti and Al are sensitive to moist conditions in the clay-forming process. In the sedimentary basin, the contents of these elements in clay are preserved and allow to infer past climates. Humid events occurred in the Dapingian, Sandbian, early Katian and Hirnantian (Ordovician) and in the Middle and Late Llandovery (Silurian). Juxtaposition with the sea-level curve shows correlation of five humid climate intervals with eustatic transgressions, suggesting global causes for these climatic changes. The warm and humid events, lasting one to two million years, occurred as climaxes between ice ages. An exceptional humid event within the Hirnantian glacial time occurs during mid-Hirnantian transgression, *i.e.* at a time of relative warming, as well.

1. Introduction

The cyclic alternation of sediments in geological sections has inspired geologists to find the reasons and create different models to illustrate the phenomenon. Oscillation of the sea level generating transgressions and regressions explains the variation of layers of either different grain size or lithological-mineralogical composition (Johnson, 2006; Haq and Schutter, 2008). The alternation of limestone–marlstone involves climatic reasons; the model by Jeppsson (1990) and (Aldridge et al., 1993) describes repeated arid–humid conditions and related changes in oxic–anoxic state of the ocean. After intensive studies of isotopes, particularly of $\delta^{13}C$ and $\delta^{18}O$, a hypothesis was proposed that a number of ice ages had occurred in the Palaeozoic (Azmy et al., 1998; Saltzman and Young, 2005; Saltzman, 2005; Kaljo et al., 2003). In the present study we track the climatic changes recorded in the clay fraction and concentrate on the relationship between humid climatic events and high sea-levels. We focus on the distribution of Rb, Zr, Nb, Ti and Al in the Dapingian–Llandovery geological sections, covering the time from 470 to 435 Ma. The sedimentary rock of the East Baltoscandian Basin, which has received the terrigenous clay from the Fennoscandian Shield, is the source material for investigation.

2. Geological background

The Fennoscandian Shield is situated adjacent to the NE Baltoscandian Basin (Fig. 1). Precambrian rocks of the shield represent the average composition of the continental Earth's crust. The parent rock for chemical weathering consists of metamorphosed schists and gneisses, granitic plutons and smaller mafic bodies (Simonen et al., 1997). The Fennoscandian Shield is flat and the sediment reaching the basin fine-grained, consisting of clay and silt. Limestones and marlstones are the lithological types of the shallow shelf, while in the deep shelf more clayey sediments occur. Illite is the main clay mineral in the shallow shelf (Põlma, 1982). Possible precursor minerals to illite, such as vermiculite, have not been detected. During the Ordovician and Silurian, the Baltic Craton drifted from temperate latitudes towards the Equator (Torsvik et al., 1996; Cocks and Torsvik, 2005). Several glaciations at the South Pole took place at that time. Positive excursions of $\delta^{13}C$ and great gaps in sediments of the shallow shelf reflect the glaciations and sea-level drops (Kiipli et al., 2010; Loi et al., 2010). The time between ice ages can be considered as a warmer period with a higher sea level.

3. Geochemical background

3.1. Formation of Rb, Ti, Nb and Zr in clays

During chemical weathering and the following erosion on large areas the source material is homogenised and achieves the aver-

* Corresponding author.
E-mail address: tarmo.kiipli@ttu.ee (T. Kiipli).

http://dx.doi.org/10.1016/j.chemer.2017.05.002
0009-2819/

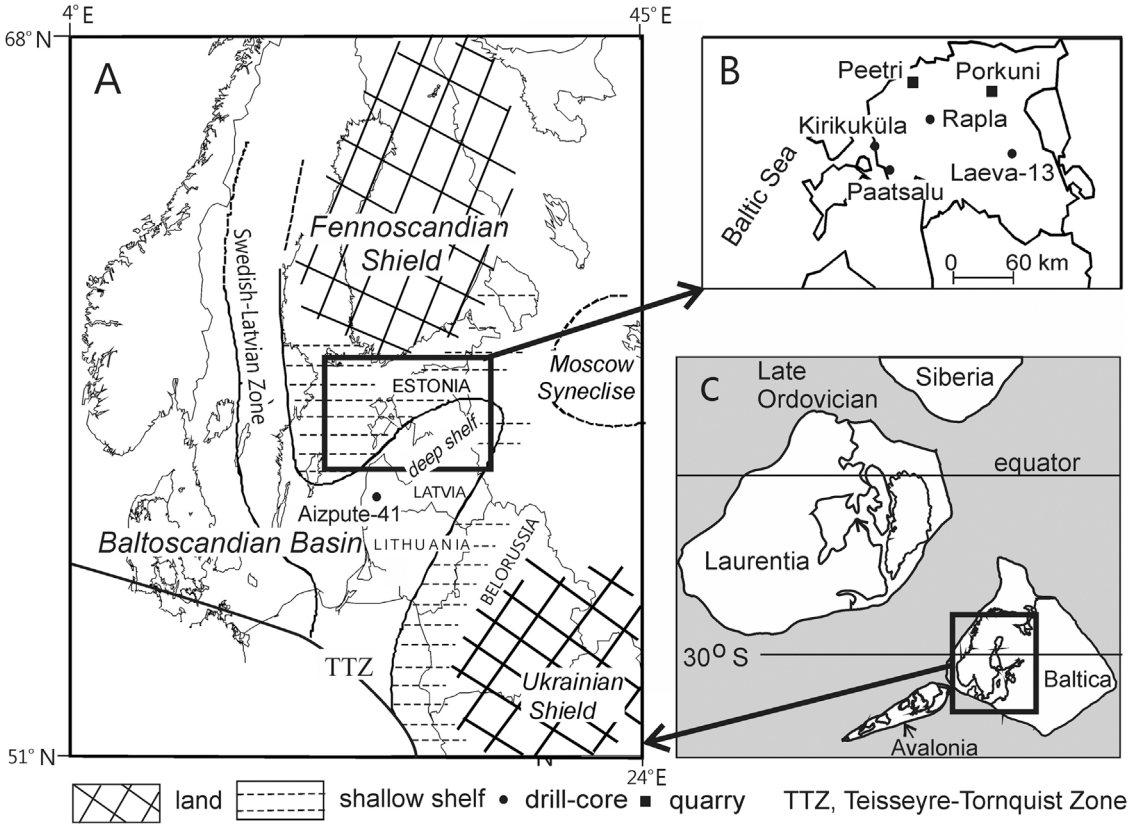

Fig. 1. A sketch-map of the Baltic Palaeozoic Sedimentary Basin (A), sampled cores and quarries in Estonia (B) and Late Ordovician palaeogeography (C) composed according to Cocks and Torsvik (2005), Golonka et al. (2003) and Nikishin et al. (1996).

age chemical composition corresponding to the climate of the particular time. Beside landscape and composition of the parent rock, the temperature and humidity are the most important factors affecting clay composition (Van de Kamp, 2010). In the sedimentary basin, terrigenous clay minerals preserve many signatures obtained during chemical weathering, among others, Al, Rb, Ti, Nb and Zr. The contents of Rb, Ti, Nb, Zr and Al in clay depend on humidity and temperature conditions, as can be inferred from laboratory experiments and recent weathering profiles. Akul'shina (1976), after investigating different geological sections, including the formations with coal interbeds pointing to humid climate, and evaporates assigned to arid climate, elaborated an empirical relationship between Al_2O_3/TiO_2 of clay and climate. The Al_2O_3/TiO_2 ratio below 20 shows humid climate, the ratio over 30—arid, and the values between 20 and 30 refer to semi-humid and semi-arid climates. When using the reciprocal ratio, TiO_2/Al_2O_3, as done in the present study, the value >0.05 points to humid conditions. The increase in the TiO_2/Al_2O_3 ratio of clay at wet climate is explained by higher removal rates of Al from the parent rock at the first stages of chemical weathering. The proportion of Ti increases and Ti is readily incorporated into the new-formed clay, into a tetrahedrally coordinated position (Cornu et al., 1999). Nb and Zr can have similar valence state and an ion radius close to that of Ti, thereby they behave similarly in the clay-forming process. Though Al, Ti, Zr and Nb are generally immobile (Nesbitt et al., 1980; Kiipli et al., 2017), differences in mobility occur; aluminium goes into solution first and Zr is the least mobile of the four (Hodson, 2002). In diagenesis, the mobility of Ti is possible. The anatase found in the clay fraction is very likely related to muscovite or illite and forms in post-depositional processes. Alló (2004) describes the in situ formation of TiO_2 minerals in a non-metamorphised Precambrian sedimentary clay. The TiO_2 minerals have been found in association with the faces (001) of illite flakes or in the pores between flakes, suggesting that Ti originates from clay minerals (Alló, 2004). The co-occurrence of Rb with Ti, Nb and Zr is somewhat unexpected, as Rb^+ is a mobile ion moving easily into solution with Na^+ at the first stages of chemical weathering. Previous studies of Rb, mostly linked to Cs and radiocaesium as radioactive wastes, have shown that Rb and Cs have similarities in sorption into illitic clay (Brouwer et al., 1983). High concentrations of Rb have been recorded in soils of the Savannah River Site, North America. These soils are products of substantial weathering of coastal plain sediments at warm climate and relatively high rainfalls. Elevated Rb contents in these soils have been assigned to hydroxy-interlayered vermiculite (Wampler et al., 2012), a precursor mineral to illite. In Toorongo, east-central Victoria, Australia, the most leached part of the weathering profile also reveals increased Rb contents in residues inherited from the alteration biotite → vermiculite → illite (Nesbitt et al., 1980). Rubidium dissolves readily from the parent rock when the climate turns wet, and adsorbs into the newly-formed clay mineral. Weathered mica particles have suitable sites for Rb^+ fixation in the expanded interlayers of the frayed edges (Zachara et al., 2002; Wampler et al., 2012). The fixation capacity of the frayed edges is regulated by hydroxy-Al polymers (Maes et al., 1999; Meunier, 2007) whose intrusion into crystal structure is sensitive to humidity as well (Nakao et al., 2009a, 2009b).

4. Materials

To ensure that we study comparable material in tracking the climate through the long geological time, the material was collected from Estonian cores of the shallow shelf. Since the deeper part of the Baltoscandian Basin has received sediments from weathering areas of other climate regimes and of different mineral composi-

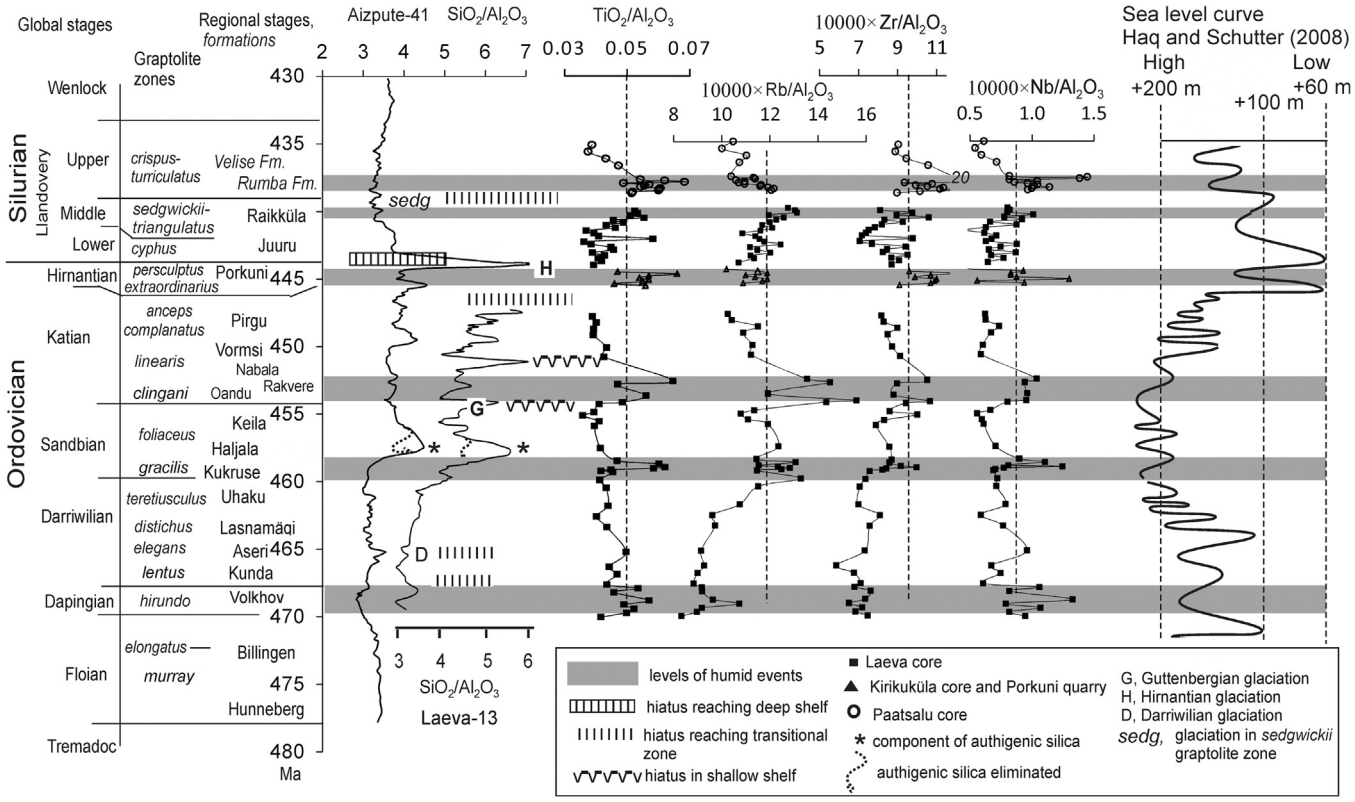

Fig. 2. Sea-level stands *vs.* humid events. The whole-rock SiO_2/Al_2O_3 3-point average is a proxy for sea level fluctuations in the deep (the Aizpute core) and shallower shelves (the Laeva core). The sea-level curve by Haq and Schutter (2008) is given. Al_2O_3-normalised TiO_2, Rb, Zr and Nb of the clay fraction of the composite core section show elevated values at certain stratigraphical levels, the levels of humid events (HE) (grey ribbons). Correlation of the Ordovician global and regional stages and graptolite zones after Nõlvak et al. (2006); Silurian correlations after Nestor (1997) and Kiipli et al. (2006).

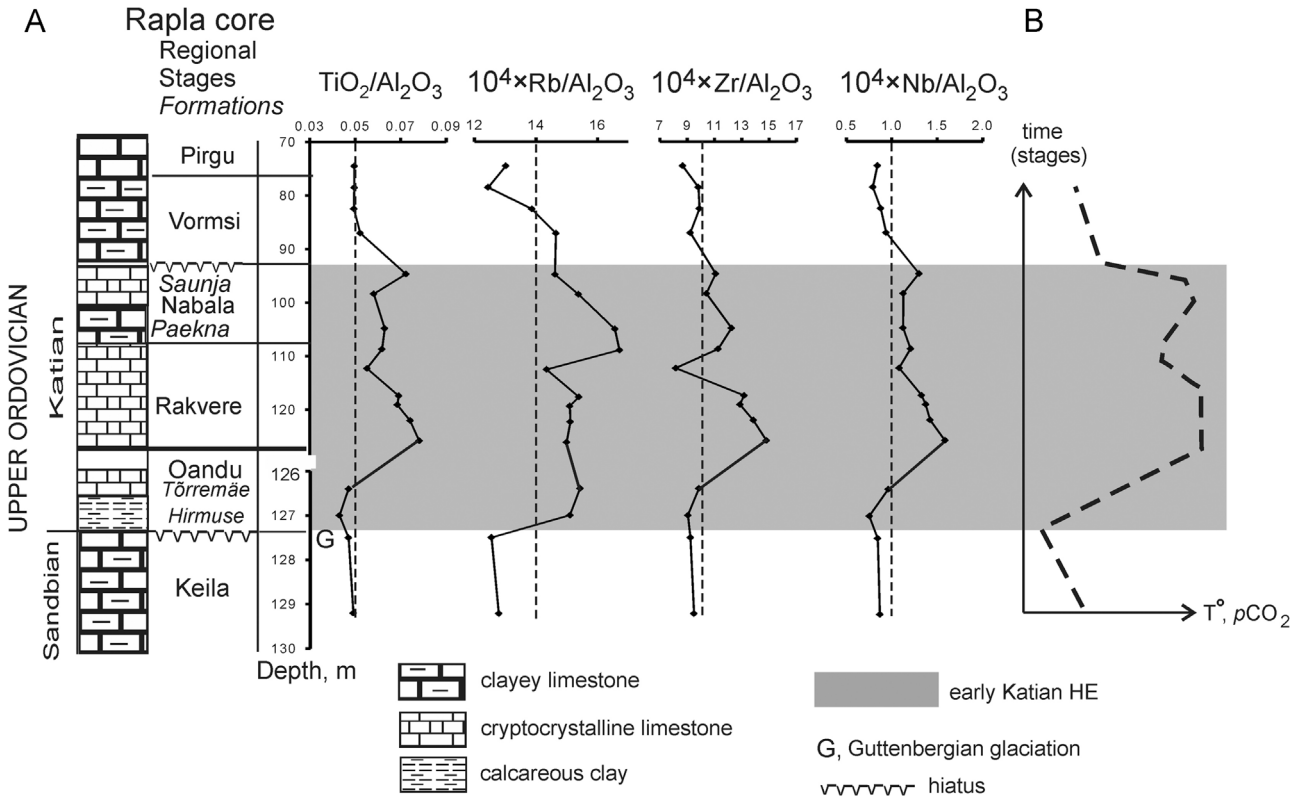

Fig. 3. The Rapla core. (A) Lithology and Al_2O_3-normalised TiO_2, Nb, Rb and Zr of the clay fraction of the lower Katian HE. Note the change in the vertical scale at the Oandu/Rakvere boundary. (B) development of temperature and pCO_2 inferred from the elements and lithology.

tion (Kiipli et al., 2008, 2009), this part was omitted. For tracking the humidity we used only the clay fraction, as variations in the composition and quantity of coarser fractions could have brought about uncertainty (Kiipli et al., 2012). The bulk of samples came from the Laeva-13 (hereafter simply *the Laeva)* core, which is situated at the upper boundary of the transitional zone between the shallow and the deep shelf (Fig. 1). The Laeva section is rather complete, though some stratigraphic intervals are condensed or absent. To complement the lacking parts, the clays from the Porkuni quarry and Kirikuküla core for the Hirnantian, and Paatsalu core for the Upper Llandovery, were used (Fig. 2). In addition, a trench in the Peetri Hillock (Supplementary Table 1) and the Rapla core were investigated for the clay composition of the Sandbian and lower Katian (Fig. 3). The whole-rock samples of the Aizpute-41 (hereafter simply *the Aizpute*) and Laeva cores were analysed for SiO_2/Al_2O_3 ratio.

5. Methods

The clay fraction <1 μm was separated from the carbonate rock devoid of organic carbon. The carbonate samples were then treated with 1N HCl, considering that for 100 g calcite 2 L of acidic solution was needed. The insoluble residue, consisting of clay and silt with minor sand, was settled for 24 h in a 10-cm-thick column of 0.1% Na-pyrophosphate solution. The unsettled part, the clay fraction <1 μm, was centrifuged, washed and dried. Thereafter, the pressed clay pellets were subjected to the XRF analysis. The concentrations of elements and crystal water were calculated using the standard "MultiRes" and "Eval 2" software programmes from Bruker AXS. The relative standard deviation of major components was 0.2–0.9% (calculated from repeated measurements of the in-house reference material Es-1). The detection limit for the main elements heavier than P was 0.01%, for lighter elements—0.1%. The precision of Rb was ±4 ppm, of Nb ±1.5 ppm and of Zr ±6 ppm (two standard deviations). The normalisation by Al_2O_3 was used to exclude any influence of changes in contents of other main elements. The mineral composition of the clay fraction was analysed in more than 20 samples from different cores using the X-ray diffractometry (XRD). The measurements were carried out in the Bruker D8 Advance diffractometer using Fe-filtered Co radiation and LynxEye detector. The whole-rock composition, used for calculating the SiO_2/Al_2O_3 ratio was analysed from pressed powder pellets in the Bruker AXS S-4 spectrometer. The 3-point averages of SiO_2/Al_2O_3 of the Aizpute core from the deep and Laeva core from the shallower shelf were used to describe the sea-level fluctuations (Fig. 2). Grain size of the siliciclastic part of 32 Laeva samples was measured using the sedigraph Horiba LA-950. The mean grain size was automatically calculated according to the formula $MGS = \Sigma\, q \cdot ø/100$, where q was the percentage of a particular grain fraction and ø the diameter of grains (in μm) in this fraction. The mean grain size vs. SiO_2/Al_2O_3 ratio was used to assert the whole-rock SiO_2/Al_2O_3 as a proxy for sea-level stand.

6. Results

6.1. Minerals of the clay fraction of the sedimentary rock

Investigation of the clay fraction detected illite as the main mineral that also included minor muscovite polytype 2 M_1. Terrigenous quartz and orthoclase, together around 10%, were also present. The content of chlorite varied from 0.5 to 6%, being higher in the Silurian clay. *In situ* formed corrensite, up to 30%, occurred in the upper Pirgu (uppermost Katian) and Porkuni (Hirnantian) stages, mainly in cores between the shallow and the deep shelf. In the lower Haljala Stage (lower Katian), the authigenic chert originating from the silica sponge *Pyritonema* (Männil, 1966) was present in both deep and shallow shelves, in the clay as well as in coarser fractions. Fine dispersed pyrite was predominant in the grey-coloured and hematite–goethite in the red beds. The clay of the Rakvere Stage of the Rapla core contained a few percent of authigenic K-sanidine and 0.5% of anatase.

6.2. Intervals of the increased Al-normalised Rb, Ti, Zr and Nb—the HEs

Geological sections in Estonia show elevated Al_2O_3-normalised values of Rb, Zr, Nb and TiO_2 of the clay fraction in four Ordovician and two Silurian stages. As Rb, Zr, Nb and Ti are sensitive to moist conditions, we call the levels of their increased contents in geological sections, the levels of humid events (HEs). The oldest level of a HE is in the Volkhov Stage, Dapingian, Middle Ordovician (Fig. 2). The interval reveals high TiO_2/Al_2O_3 and Nb/Al_2O_3, but low Zr/Al_2O_3 and Rb/Al_2O_3 ratios. The following, Sandbian interval starts with a high Rb/Al_2O_3 ratio in the middle of the Kukruse Stage and ends with peaks of TiO_2/Al_2O_3, Zr/Al_2O_3 and Nb/Al_2O_3 in the upper Kukruse. The Peetri Hillock near Tallinn (capital city of Estonia) reveals similarly high values in the correlative section (Supplementary Table 1). The time-span between the first and second HE is approximately 9 Ma. The third HE starts about 4–5 Ma later in the early Katian, comprising the Oandu, Rakvere and Nabala regional stages (Fig. 2). The Rakvere Stage exhibits the highest absolute and Al_2O_3-normalised Rb values. The content of Rb in the Rapla core reaches 328 ppm, with the mean around 300 ppm within the HE, and 220–250 ppm as the background value outside the HE (Fig. 3). The Hirnantian HE shows high Al_2O_3-normalised values of Zr, Nb and TiO_2, but not of Rb (Fig. 2). The HE of the Raikküla Stage (Middle Llandovery, Silurian) follows the post-glacial Early Llandovery with fluctuating element-to-Al ratios. A gap in sedimentation separates the Middle Llandovery event from the overlying Late Llandovery. In the Paatsalu core (Fig. 2), the HE of the Late Llandovery, corresponding to the Rumba Formation of the Adavere Stage, reveals the highest Zr and Nb contents, 413 ppm and 29 ppm, correspondingly (Supplementary Table 1). Very often the appearance of element maxima within a HE is asynchronous—the Rb/Al_2O_3 peak occurs first, other elements following later on (Fig.-s 2, 3).

7. Discussion

7.1. The whole-rock SiO_2/Al_2O_3 curve as a proxy for sea-level stand

The whole-rock SiO_2/Al_2O_3 and mean grain size of the siliciclastic component reveal a positive correlation ($R^2 = 0.44$) in the Laeva core, enabling the use of SiO_2/Al_2O_3 as proxy for the grain size (Fig. 4) and sea level. The mean grain size is larger when the coastal denudation area is closer to the core site, pointing to regression, while smaller grain size corresponds to transgression. The Laeva core shows higher SiO_2/Al_2O_3 peaks than the more clayey Aizpute section (Fig. 2), as in the cores of shallower facies the addition of coarser fractions with abundant quartz raises the SiO_2/Al_2O_3 value at regressions. The mid-Sandbian authigenic chert masks the terrigenous SiO_2/Al_2O_3 ratio. To eliminate the influence of chert and to correct the sea-level curve, the distribution of whole-rock TiO_2/Al_2O_3 was used. Ti as a terrigenous component reveals no peak in the Haljala Stage pointing to the absence of a great regression (Fig. 2). The juxtaposition of Al_2O_3-normalised elements of clay and SiO_2/Al_2O_3 ratio of the whole-rock shows correlation between most HEs and maximum sea-level stands (Fig. 2). Comparison of the regional sea-level curve (represented by SiO_2/Al_2O_3

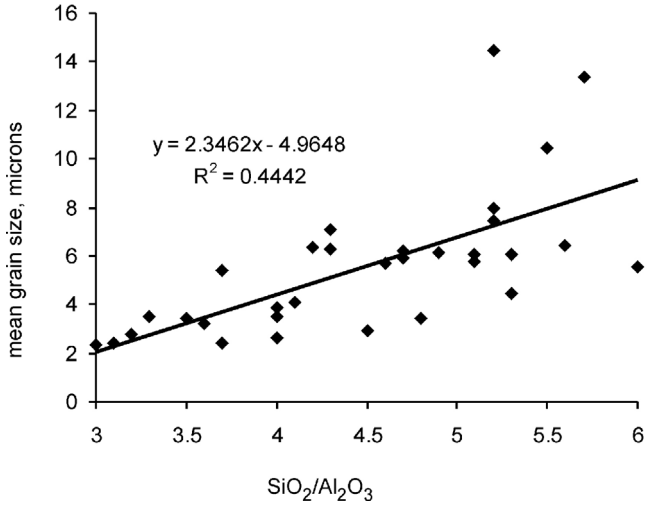

Fig. 4. Mean grain size *vs.* SiO_2/Al_2O_3 of the Laeva core.

ratio) with the global sea-level curve by Haq and Schutter (2008) (Fig. 2) reveals a rather good correlation. Some disagreements may arise from regional differences or correlation problems. A review of other Ordovician and Silurian sea-level curves by several authors is given by Munnecke et al. (2010).

7.2. Eustatic transgressions and humid events

The HEs reveal short-term but prominent changes in climate and chemical weathering lasting approximately one to two million years. In the Baltoscandian Basin, the levels of the increased Ti, Rb, Zr and Nb, *i.e.* the HEs, correspond to the short-time maxima within longer sea-level highstands, according to both regional and global curves (Fig. 2). The sea-level rise can be either eustatic or tectonic-related regional. If the HE corresponds to eustatic transgression, the global cause for the HE formation is very likely. The melting of ice caps at the South Pole, due to increase in temperature, would induce eustatic transgressions. The rise in temperature would enhance evaporation and rainfalls, making the climate humid (Rind, 2000). The increased contents of Ti, Rb, Zr and Nb in illite are well expressed in the medium latitudes. In the equatorial zone, the result might be different. Minerals forming at very humid conditions, such as kaolinite, have no suitable sites in crystal lattice to incorporate elements, *e.g.* Rb.

The Volkhovian (Dapingian) sea-level maximum is a culmination of the transgression proceeding since the Floian, as recorded in the Baltoscandia (Männil, 1966 figs. 50–52), or since the Early Cambrian on the global scale (Haq and Schutter, 2008). The maximum sea stand, expressed by the lowest SiO_2/Al_2O_3 values in the sea-depth curve of the Aizpute core, is correlative with a HE (Fig. 2). Further on, in the Darriwilian, the increase in $\delta^{18}O$ apatite shows cooling of the atmosphere and sea water (Trotter et al., 2008). The corresponding rise in SiO_2/Al_2O_3, seen in the Aizpute curve (Fig. 2), marks the Darriwilian regression and possible glaciation. The next, early Sandbian HE of the Kukruse Stage corresponds to the phase of the highest sea-level stand of the Palaeozoic (Haq and Schutter, 2008). The following Guttenbergian glaciation, correlative with the *Diplacanthograptus caudatus* (in USA), *Dicranograptus clingani* (in Baltica) or *Climacograptus bicornis* (in Argentine) graptolite zones (Bergström et al., 2009; Loydell, 2012; Sial et al., 2013), separates the Sandbian and Katian HEs. In the Laeva core, the Guttenbergian glaciation is expressed as a steep increase in SiO_2/Al_2O_3 values in the late Keila Stage (Fig. 2). On the SiO_2/Al_2O_3 curve of the Aizpute core, the glaciation is poorly followed due to a condensed interval or hiatus. The beginning of the Katian HE is contemporaneous with the post-Guttenbergian transgression of the Oandu Stage (middle *clingani*). In the Belarussian part of the Baltoscandian Basin, the Oandu strata cover the Cambrian sediments unconformably, pointing to a transgression (Ropot and Pushkin, 1987). In Estonia, the areal spread of the lower Oandu Stage is patched (Männil, 1966), probably indicating a developing sea-level rise after the Guttenbergian lowstand. The overlying Rakvere Stage shows a high-sea stand, as wide areas in Estonia and adjacent Russia reveal similar cryptocrystalline limestone (Männil, 1966 Fig. 62). The following Nabala Stage ends with karst pointing to regression (Calner et al., 2010). Consequently, the Katian HE corresponds to the eustatic sea-level highstand after the end of Guttenbergian glaciation. The overlying Vormsi Stage, though being transgressive in Estonia, reveals no increased values of Ti, Rb, Zr and Nb (Fig. 3). The Hirnantian is a time of ice age and increased values of $\delta^{13}C$ and $\delta^{18}O$ in geological sections (Brenchley et al., 1994). In Nevada, two widespread unconformities—one at the beginning of the *extraordinarius* graptolite and *taugordeau* chitinozoan zones and the second somewhat later at the beginning of the *hassi* conodont zone—are recorded, representing glacial episodes. Carbonate deposition in shallow shelves is coeval with the interglacial between the unconformities (Bergström et al., 2014). In NE Spain, the sediments between gaps also indicate temporary warmings and transgressions within the Hirnantian (Subías et al., 2015). In the Baltoscandian Basin, regression and gaps reach the transitional zone and even the deep shelf (Ulst et al., 1982) (Fig. 2). The preserved calcareous and dolomitic sediments and small bioherms of the Porkuni Stage in Estonia point to modest transgressions and temporary warmings, similarly to the interglacial sediments of USA and Spain. High contents of Al_2O_3-normalised TiO_2, Zr and Nb, excluding Rb, occur in the clay fraction pointing to humidity in the Porkuni time (Fig. 2). As an alternative to the idea on temporary warming, the rainfalls could result from the equatorward shift of the polar front to the latitudes near 30°S, inferred from the movement of cold-water faunas into lower latitudes (Vandenbroucke et al., 2010). All these facts are suggestive of oscillating climate in the Hirnantian.

In the early Silurian, sea-level rise prevailed (Fig. 2). The high sea stand was temporarily interrupted by regressions. A gap in Estonian sections, corresponding to the *Stimulograptus sedgwickii* graptolite zone of the upper Middle Llandovery, and the correlative positive carbon isotope excursion in Canada (Melchin and Holmden, 2006), could be indicative of a glaciation event. Two HEs occur in the Llandovery—the first in the Raikküla Stage of the Middle Llandovery and the second in the Rumba Formation of the Adavere Stage (Late Llandovery). The *sedgwickii* gap between them shows that the climate state could have changed rapidly from warm and humid to cold and back again. Since the latest Llandovery, the Fennoscandian Shield has been situated in arid latitudes. The clay minerals, though mainly illites (Kiipli et al., 2016), reveal no increase in the contents of Ti, Rb, Zr and Nb, *i.e.* lack any indication of a HE. The climate of arid latitudes together with the peculiarities of the emerging Caledonides in the vicinity, probably, impeded the revelation of possible global humid events.

Jeppsson's model (1990) on arid–humid climatic alternation, based on marlstone–limestone variation in Gotland initiated a hot debate in 1990s. According to Jeppsson (1990), humid climate in low latitudes and cold climate in high latitudes corresponds to marly sequences, while dry climate in low latitudes and warm climate in high latitudes are coeval with carbonate-rich sequences. Once isotope data was included, the $\delta^{18}O$ and $\delta^{13}C$ had various interpretations by different authors. The high isotope values paralleled with carbonate-rich units point to either increase in ocean water salinity and faster organic carbon burial rate (Bickert et al., 1997), or lower ocean water temperatures and higher primary productivity in ocean surface waters (Wenzel and Joachimski, 1996). The marlstones, considered as belonging to humid episodes by

Jeppsson (1990), correspond to the depleted isotope values (Bickert et al., 1997; Wenzel and Joachimski, 1996). In the last few decades, several authors (Brenchley et al., 1994; Bergström et al., 2010; Kiipli et al., 2010) have acclaimed a link between high isotope values, low temperature, regression and glaciation. The present study operates mainly with sea-levels and humid events using the initial idea of arid–humid alternation of climate by Jeppsson (1990).

7.3. *Inferring the climate from lithology and trace elements*

The succession of chemical elements and changes in lithology can indicate related developments of climate during a HE. Fig. 3 illustrates the lower Katian case on the basis of the Rapla core. The section reveals no elevated TiO_2, Rb, Nb and Zr Al_2O_3-normalised values in clays of the Keila Stage before the Guttenbergian glaciation (Fig. 3A). The first peak of Rb/Al_2O_3 occurs in the Oandu Stage pointing to formation of warm and moist climate after the ice age, as the increase in temperature generated evaporation and rainfalls (Fig. 3B). The Oandu Stage consists of claystone and marlstone in the shallow shelf. The rise in pCO_2 growing in pace with the temperature caused low pH and poor carbonate formation. In the overlying Rakvere Stage, the TiO_2, Nb and Zr Al_2O_3-normalised values increase, indicating great humidity. Instead of former clayey sediments, pure cryptocrystalline limestone occurs. The pH increase of seawater, which favours limestone formation, is maintained by decline in CO_2, either global or local. In the latter case, the pH rise could be due to local increase in primary bioproductivity utilizing CO_2, without changing the temperature. Though, no clear evidences for bioproductivity rise have been found in the Rakvere Stage. Decrease in atmospheric pCO_2 presumes corresponding lowerings in temperature, which contradicts the high humidity of the Rakvere time. We propose that stabilisation or minor decrease in temperature and pCO_2 occurred (Fig. 3B). The temperature stayed high enough to generate evaporation and humidity, the end of rise in pCO_2 increased seawater pH favouring the rapid formation of limestone. In the following Nabala time, the small fluctuations of temperature and CO_2 recurred. At the end-Nabala time, the possible decline in temperature and evaporation led to decrease in element contents and cease of the HE.

8. Conclusion

Rb, Zr, Nb and Ti and their Al_2O_3-normalised values of the clay fraction reveal considerable increase at several stratigraphical levels in the Baltoscandian Basin. The mentioned elements are sensitive to humidity and incorporated into illitic clay in the process of chemical weathering in the adjacent land. Thus, in the marine sedimentary sections, the levels of increased contents of these elements are called 'humid events' (HE). HEs occurred in the Dapingian, Sandbian, Katian and Hirnantian (Ordovician) and in the Middle and Upper Llandovery (Silurian). Juxtaposition of HEs with the sea-level curve shows correlation of HEs with the highest eustatic sea stands, indicating warm ice-free times. Hirnantian humidity is an exception, occurring either, due to the latitudinal shift of climate during glaciation, or warming and sea-level rise during the interglacial in the mid-Hirnantian. The development of climatic conditions within a HE can be inferred from the order of appearance of high values of the studied elements and comparison with coeval lithology. A HE often starts with an increase in Rb/Al_2O_3 pointing to humid and warm conditions, followed by rise in Zr, Nb and Ti contents emphasizing humidity.

In addition to the cold glaciation intervals established by previous researchers, several warm and humid short-stands occur as humid climaxes between ice ages, lasting one to two million years.

Acknowledgments

This study is financed by the Department of Geology at Tallinn University of Technology. The article is a contribution to the projects IGCP 652 and IGCP 653. We thank H. Pohl-Raidla and M-L. Kiipli for the linguistic help. We are grateful to two anonymous reviewers. The rock samples come from the collection of the Department of Geology at Tallinn University of Technology.

Appendix A. Supplementary data

Supplementary data associated with this article can be found, in the online version, at http://dx.doi.org/10.1016/j.chemer.2017.05.002

References

Akul'shina, E.P., 1976. Methods for determining weathering conditions, sedimentation and post-sedimentary transformations according to clay minerals. In: Akul'shina, E.P. (Ed.), Clay Minerals as Indicators of Rock Forming Conditions. Novosibirsk, Nauka, pp. 9–37 (in Russian).
Aldridge, R.J., Jeppsson, L., Dorning, K.J., 1993. Early silurian oceanic episodes and events. J. Geol. Soc. 150, 501–513.
Alló, W., 2004. Authigenic Ti-bearing crystals in a Precambrian clay from Buenos Aires province, Argentina. Clays Clay Mineral. 52, 304–310.
Azmy, K., Veizer, J., Bassett, M.G., Copper, P., 1998. Oxygen and carbon isotopic composition of Silurian brachiopods: implications for coeval seawater and glaciations. GSA Bull. 110, 1499–1512.
Bergström, S.M., Xu Chen Gutierrez-Marco, J.C., Dronov, A., 2009. The new chronostratigraphic classification of the Ordovician system and its relations to major regional series and stages and to $\delta^{13}C$ chemostratigraphy. Lethaia 42, 97–107.
Bergström, S.M., Young, S.A., Schmitz, B., 2010. Katian (Upper Ordovician) $^{\delta 13}C$ chemostratigraphy and sequence stratigraphy in the United States and Baltoscandia: a regional comparison. Palaeogeogr. Palaeoclimatol. Palaeoecol. 296, 217–234.
Bergström, S.M., Eriksson, M.E., Young, S.A., Ahlberg, P., Schmitz, B., 2014. Hirnantian (latest Ordovician) $\delta^{13}C$ chemostratigraphy in southern Sweden and globally: a refined integration with the graptolite and conodont zone successions. GFF 136, 355–386.
Bickert, T., Pätzold, J., Samtleben, C., Munnecke, A., 1997. Paleoenvironmental changes in the Silurian indicated by stable isotopes in brachiopod shells from Gotland, Sweden. Geochim. Cosmochim. Acta 61, 2717–2730.
Brenchley, P.J., Marshall, J.D., Carden, G.A.F., Robertson, D.B.R., Long, D.G.F., Meidla, T., Hints, L., Anderson, T.F., 1994. Bathymetric and isotopic evidence for a short-lived Late Ordovician glaciation in a greenhouse period. Geology 22, 295–298.
Brouwer, E., Baeyens, B., Maes, A., Cremers, A., 1983. Cesium and rubidium ion equilibria in illite clay. J. Phys. Chem. 87, 1213–1219.
Calner, M., Lehnert, O., Nõlvak, J., 2010. Palaeokarst evidence for widespread regression and subaerial exposure in the middle Katian (Upper Ordovician) of Baltoscandia: significance for global climate. Palaeogeogr. Palaeoclimatol. Palaeoecol. 296 (3-4), 235–247.
Cocks, L.R.M., Torsvik, T.H., 2005. Baltica from the late Precambrian to mid-Palaeozoic times: the gain and loss of a terrane's identity. Earth Sci. Rev. 72, 39–66.
Cornu, S., Lucas, Y., Lebon, E., Ambrosi, J.P., Luizão, F., Rouiller, J., Bonnay, M., Neal, C., 1999. Evidence of titanium mobility in soil profiles, Manaus, central Amazonia. Geoderma 91, 281–295.
Golonka, J., Bocharova, N.Y., Ford, D., Edrich, M.E., Bednarczyk, J., Wildharber, J., 2003. Paleogeographic reconstructions and basins development of the Arctic. Mar. Petrol. Geol. 20, 211–248.
Haq, B.U., Schutter, S.R., 2008. A chronology of paleozoic sea-level changes. Science 322, 64–68.
Hodson, M.E., 2002. Experimental evidence for mobility of Zr and other trace elements in soils. Geochim. Cosmochim. Acta 66, 819–828.
Jeppsson, L., 1990. An oceanic model for lithological and faunal changes tested on the Silurian record. J. Geol. Soc. 147, 663–674.
Johnson, M.E., 2006. Relationship of Silurian sea-level fluctuations to oceanic episodes and events. GFF 128, 115–121.
Kaljo, D., Martma, T., Männik, P., Viira, V., 2003. Implications of Gondwana glaciations in the Baltic late Ordovician and Silurian and carbon isotopic test of environmental cyclicity. Bull. Soc. Géol. Fr. 174, 59–66.
Kiipli, E., Kiipli, T., Kallaste, T., 2006. Identification of the *O*-bentonite in the deep shelf sections with implication on stratigraphy and lithofacies, East Baltic Silurian. GFF 128, 255–260.
Kiipli, E., Kallaste, T., Kiipli, T., 2008. Hydrodynamic control of sedimentation in the ordovician (Arenig—Caradoc) Baltic basin. Lethaia 41, 127–137.
Kiipli, E., Kiipli, T., Kallaste, T., 2009. Reconstruction of currents in the Mid-Ordovician–Early Silurian central Baltic Basin using geochemical and mineralogical indicators. Geology 37, 271–274.

Kiipli, T., Kiipli, E., Kaljo, D., 2010. Silurian sea level variations estimated using SiO_2/Al_2O_3 and K_2O/Al_2O_3 ratios in the Priekule drill core section, Latvia. Bolletino della Societa Paleontologica Italiana 49, 55–63.
Kiipli, E., Kiipli, T., Kallaste, T., Siir, S., 2012. Al_2O_3/TiO_2 ratio of the clay fraction of Late Ordovician –Silurian carbonate rocks as an indicator of palaeoclimate of the Fennoscandian Shield. Palaeogeogr. Palaeoclimatol. Palaeoecol. 365-366, 312–320.
Kiipli, E., Kiipli, T., Kallaste, T., Märss, T., 2016. Chemical weathering east and west of the emerging Caledonides in the Silurian—early Devonian, with implications for climate. Can. J. Earth Sci. 53, 774–780.
Kiipli, T., Hints, R., Kallaste, T., Verš, E., Voolma, M., 2017. Immobile and mobile elements during the transition of volcanic ash to bentonite—an example from the early Palaeozoic sedimentary section of the Baltic Basin. Sediment. Geol. 347, 148–159.
Loi, A., Ghienne, J.-F., Dabard, M.P., Paris, F., Botquelen, A., Christ, N., Elaouad-Debbaj, Z., Gorini, A., Vidal, M., Videt, B., Destombes, J., 2010. The Late Ordovician glacio-eustatic record from a high-latitude storm-dominated shelf succession: the Bou Ingarf section (Anti-AtlasSouthern Morocco). Palaeogeogr. Palaeoclimatol. Palaeoecol. 296, 332–358.
Loydell, D.K., 2012. Graptolite biozone correlation charts. Geol. Mag. 149, 124–132.
Männil, R., 1966. Evolution of the Baltic basin during the Ordovician. Valgus, Tallinn, pp. 201 (in Russian with English summary).
Maes, E., Iserentant, A., Herbauts, J., Delvaux, B., 1999. Fixation of radiocaesium traces in a weathering sequence mica—vermiculite—hydroxy-interlayered vermiculite. Eur. J. Soil Sci. 50, 117–125.
Melchin, M.J., Holmden, C., 2006. Carbon isotope chemostratigraphy of the Llandovery in Arctic Canada: implications for global correlation and sea-level change. GFF 128, 173–180.
Meunier, A., 2007. Soil hydroxy-interlayered minerals: a re-interpretation of their crystallochemical properties. Clays Clay Miner. 55, 380–388.
Munnecke, A., Calner, M., Harper, D.A.T., Servais, T., 2010. Ordovician and Silurian sea-water chemistrysea level, and climate: a synopsis. Palaeogeogr. Palaeoclimatol. Palaeoecol. 296, 389–413.
Nõlvak, J., Hints, O., Männik, P., 2006. Ordovician time-scale in Estonia: recent developments. Proc. Estonian Acad. Sci. Geol. 55, 95–108.
Nakao, A., Funakawa, S., Watanabe, T., Kosaki, T., 2009a. Pedogenic alterations of illitic minerals represented by Radiocesium Interception Potential in soils with different soil moisture regimes in humid Asia. Eur. J. Soil Sci. 60, 139–152.
Nakao, A., Funakawa, S., Kosaki, T., 2009b. Hydroxy-Al polymers block the frayed edge sites of illitic minerals in acid soils: studies in southwestern Japan at various weathering stages. Eur. J. Soil Sci. 60, 127–138.
Nesbitt, H.W., Markovics, G., Price, R.C., 1980. Chemical processes affecting alkalis and alkaline earths during continental weathering. Geochim. Cosmochim. Acta 44, 1659–1666.
Nestor, H., 1997. Table 8. the silurian of Estonia. In: Raukas, A., Teedmäe, A. (Eds.), Geology and Mineral Resources of Estonia. Estonian Academy Publishers, Tallinn, pp. 90–91.
Nikishin, A.M., Ziegler, P.A., Stephenson, R.A., Cloetingh, S.A.P.L., Furne, A.V., Fokin, P.A., Ershov, A.V., Bolotov, S.N., Korotaev, M.V., Alekseev, A.S., Gorbachev, V.I., Shipilov, E.V., Lankreijer, A., Bembinova, E.Y., Shalimov, I.V., 1996. Late Precambrian to Triassic history of the East European Craton: dynamics of sedimentary basin evolution. Tectonophysics 268, 23–63.
Põlma, L., 1982. Comparative Lithology of the Ordovician Carbonate Rocks in the Northern and Middle East Baltic. Valgus, Tallinn, pp. 164 (in Russian with English Summary).
Rind, D., 2000. Relating paleoclimate data and past temperature gradients: some suggestive rules. Quat. Sci. Rev. 19, 381–390.
Ropot, V.F., Pushkin, V.I., 1987. Ordovician of the Belarus. Nauka i Technica, Minsk, pp. 233 (in Russian).
Saltzman, M.R., Young, S.A., 2005. Long-lived glaciation in the Late Ordovician?:Isotopic and sequence-stratigraphic evidence from western Laurentia. Geology 33, 109–112.
Saltzman, M.R., 2005. Phosphorus, nitrogen, and the redox evolution of the Paleozoic oceans. Geology 33, 573–576.
Sial, A.N., Peralta, S., Gaucher, C., Toselli, A.J., Ferreira, V.P., Frei, R., Parada, M.A., Pimentel, M.M., Pereira, N.S., 2013. High-resolution stable isotope stratigraphy of the upper Cambrian and Ordovician in the Argentine Precordillera: carbon isotope excursions and correlations. Gondwana Res. 24, 330–348.
Simonen, A., Donner, J.J., Laikakari, I., 1997. Finland. In: Moore, E.M., Fairbridge, R.W. (Eds.), Encyclopedia of Europe and Asian Regional Geology. Chapman and Hall, London, pp. 230–236.
Subías, I., Villas, E., Álvaro, J.J., 2015. Hirnantian (Late Ordovician) $\delta^{13}C$ HICE excursion in a North Gondwanan (NE Spain) periglacial setting and its relationship to glacioeustatic fluctuations. Chemie der Erde 75, 335–343.
Torsvik, T.H., Smethurst, M.A., Meert, J.G., Van der Voo, R., McKerrow, W.S., Brasier, M.D., Sturt, B.A., Walderhaug, H.J., 1996. Continental break-up and collision in the Neoproterozoic and Palaeozoic—a tale of Baltica and Laurentia. Earth Sci. Rev. 40, 229–258.
Trotter, J.A., Williams, I.S., Barnes, C.R., Lécuyer, C., Nicoll, R.S., 2008. Did cooling oceans trigger Ordovician biodiversification?:Evidence from conodont thermometry. Science 321, 550–554.
Ulst, R., Gailite, L., Yakovleva, V.I., 1982. Ordovician of Latvia. Zinatne Riga, pp. 293 (in Russian).
Van de Kamp, P., 2010. Arkose, subarkose, quartz sand, and associated muds derived from felsic plutonic rocks in glacial to tropical humid climates. J. Sediment. Res. 80, 895–918.
Vandenbroucke, T.R.A., Armstrong, H.A., Williams, M., Paris, F., Zalasiewicz, J.A., Sabbe, K., Nõlvak, J., Challands, T.J., Verniers, J., Servais, T., 2010. Polar front shift and atmospheric CO_2 during the glacial maximum of the Early Paleozoic Icehouse. Proc. Natl. Acad. Sci. U. S. A. 107, 14983–14986.
Wampler, J.M., Krogstad, E.J., Elliott, W.C., Kahn, B., Kaplan, D.I., 2012. Long-term selective retention of natural Cs and Rb by highly weathered coastal plain soils. Environ. Sci. Technol. 46, 3837–3843.
Wenzel, B., Joachimski, M.M., 1996. Carbon and oxygen isotopic composition of Silurian brachiopods (Gotland/Sweden): palaeoceanographic implications. Palaeogeogr. Palaeoclimatol. Palaeoecol. 122, 143–166.
Zachara, J.M., Smith, S.C., Liu, Chongxuan, McKinley, J.P., Serne, J., Gassman, P.L., 2002. Sorption of Cs^+ to micaceous subsurface sediments from the Hanford site, USA. Geochim. Cosmochim. Acta 66, 193–211.